

Transient Overvoltages in Power Systems: Case of Study

Xavier Domínguez, Israel Paredes, Nataly Pozo, María Trujillo, Jorge Medina, Andrés Cuaycal
Escuela Politécnica Nacional (EPN), Quito - Ecuador.

Abstract – This paper studies the transient overvoltage response in specific points within an electric grid due to the effect of switching a capacitor bank. Two proposals are exposed to mitigate this overvoltage phenomenon, which is a common result of power factor correction by using capacitors in a system, which operates at 50 Hz. The obtained results show the performance of the mentioned solutions in a practical training case scenario.

Index Terms–Overvoltages, Power Quality, Power System Operation, Transient.

I. INTRODUCTION

Generally, there are two main causes for transient overvoltages on power systems, these are lightning discharges and switching surges. System switching transients can lead to the misoperation of a substantial part of the power system, in situations such as power factor correction, capacitor switching operations or disturbances that follow the restoration of power after an outage or load shedding [1].

Capacitor switching is one of the most problematic switching event on utility systems. This can cause severe transient overvoltages that could damage machinery or equipment. These transients can propagate into the local power system utility pass through its distribution transformers and enter into the end-user's load facilities. However, these disturbances do not involve substantial overvoltages (more than two or three per unit), but they may be very difficult to suppress because of its amount of energy [2].

For these reasons, this topic is especially important to appropriately mitigate this phenomenon with accurate criteria and protection equipment. The most typical approaches to solve this issue are the use of synchronous closing breakers with pre-insertion resistors and high-energy surge protector arresters at the end-user location to limit the magnitude of the transient voltage at the end-user bus. [3].

This document provides a clear idea on how to understand and propose solutions to this transient overvoltage phenomenon to prevent the misoperation in the power system. A practical training scenario is divided in two cases of study.

II. CASE ANALYSIS I

Fig. 1 shows the electrical system used to feed a factory, which includes the following facilities: a motor control center using High Voltage (HV) induction machines and a Low Voltage (LV) network system supplying ancillary services.

Once started, the HV motors are always operated at full load. A single step capacitor bank is used at the HV side to compensate reactive power. The capacitor bank is connected a few seconds after the second motor begins its operation. On the assumption that the LV network is not connected, the maximum transient overvoltage value at the 10 kV Point of Common Coupling (PCC) can be determined.

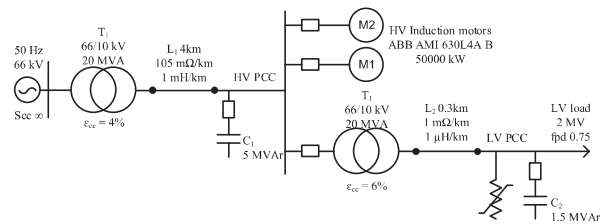


Fig. 1 Electrical system for the studied case [2]-[4]

A. Electric System Model

In order to analyse the transient voltage response due to the effect of switching the 5 MVAR capacitor bank, the electric system was modelled (assuming the low voltage network disconnected) by means the single-phase equivalent circuit referred to the 10kV side. The high voltage motor parameters for the simulation were obtained from ABB HV induction catalogue for the AMI 630L4AB/5000kW motors. They can be found in Table 1:

TABLE I
AMI 630L4AB/5000KW MOTOR CHARACTERISTICS [2]

Parameter	Value
Efficiency	96.7%
Power	5000 kW
Nominal Line Voltage	10 kV
Power factor	0.9

Knowing the Mechanical Power (P_{mech}) and the Efficiency (η), the Electrical Power (P_{elec}) consumed by the machine can be obtained with equation (1):

$$P_{elec} = \frac{P_{mech}}{\eta} = 5170.63 \text{ kW} \quad (1)$$

Hence, phase currents are given by equation (2):

$$I_{phase} = \frac{P_{phase}}{V_{phase} * pf} = 331.69 \text{ A} \quad (2)$$

Thus, the phase motor's impedance (Z_m) is given by equation (3):

$$Z_m = \frac{V_{\text{phase}}}{I_{\text{phase}}} = 10.40 \Omega \quad (3)$$

As the power factor is 0.9 ($\varphi=25.84^\circ$), the resistance of the motor (R_m) and the reactance (X_m) are presented in equations (4) and (5) respectively:

$$R_m = (Z_m)\cos(\varphi) = 15.66 \Omega \quad (4)$$

$$X_m = (Z_m)\sin(\varphi) = 7.58 \Omega \quad (5)$$

On the other hand, the inductance of the motor (L_m) is obtained following equation (6):

$$L_m = \frac{X_m}{2\pi f} = 24.1 \text{ mH} \quad (6)$$

In order to obtain the high voltage capacitor parameters, the phase current flowing through the capacitor and its capacitance are given by equations (7) and (8):

$$I_{\text{phase}_c} = \frac{Q_{\text{phase}_c}}{V_{\text{phase}}\sin(90^\circ)} = 866.02 \text{ A} \quad (7)$$

$$C_{\text{HV}} = \frac{I_{\text{phase}_c}}{2\pi f * V_{\text{phase}}} = 159.15 \mu\text{F} \quad (8)$$

Otherwise, the parameters of a transformer of 20 MVA such us reactance (X_{TX_20}) and leakage inductance (L_{TX_20}) are obtained using equation (9) and (10). In these parameters the resistance of the transformer was neglected.

$$X_{\text{TX}_20} = \frac{V_{\text{line}}^2}{S_{\text{SC}}} \epsilon_{\text{cc}} = 200 \text{ m}\Omega \quad (9)$$

$$L_{\text{TX}_20} = \frac{X_{\text{TX}_20}}{2\pi f} = 636.61 \text{ uH} \quad (10)$$

In the high voltage line impedance, according to Fig. 1, the line resistance and inductance have values of 42 m Ω and 0.4 mH respectively [1]-[6]. Moreover, in Fig. 2 can be observed the per-phase equivalent circuit implemented in Simulink-Matlab[®] using the obtained parameters.

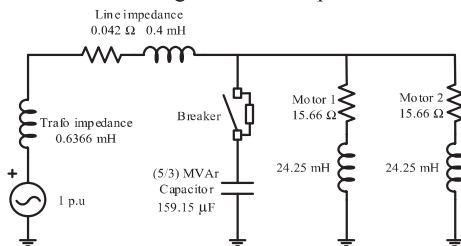


Fig. 2 Per-phase equivalent circuit implemented.

B. Transient Voltage response

Once all the parameters have been obtained, it is necessary to analyse the transient voltage response due to the capacitor switching at the High Voltage Point of Common Coupling (HV PCC) [2]-[5]. However, it must be noticed that depending on the point of wave where the switching action takes place, different transient

overvoltage responses will be obtained. In Fig. 3, it is shown the voltage response for switching the capacitor at two different moments at PCC [10].

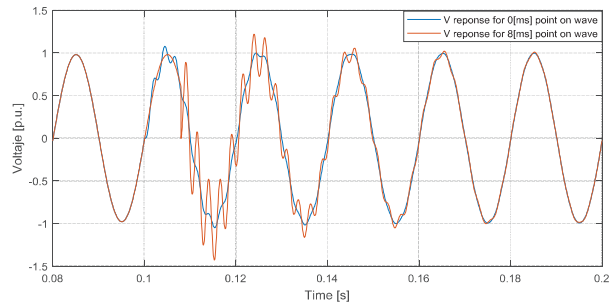


Fig. 3 Voltage response for two different switching periods

As can be seen in Fig. 3, the wave period is 20 ms because the system operates at 50 Hz. In order to find an acceptable degree of accuracy the switching point on wave that leads the worst transient response with the highest overvoltage, 40 simulations were performed for the system using steps of 0.5 ms on wave switching time. Then, the highest peak overvoltage values from each simulation will be compared so that the global maximum voltage response with the worst condition can be obtained.

The study case showed that the worst transient response has a peak value of 1.9065 p.u. and it occurs when the capacitor switching takes place at a point on wave of 4.5 ms as can be seen in Fig. 4.

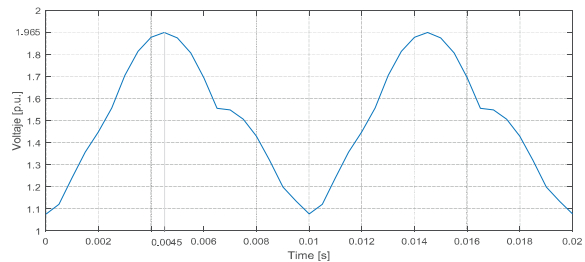


Fig. 4 Maximum p.u. voltages obtained as a function of point-on-wave capacitor switching.

The particular voltage response for this worst-case condition can be seen in Fig. 5. On the other hand, as the peak current in steady state (reference base value) can be obtained, the p.u. current response as a function of the point on wave switching instant can also be obtained by dividing the current throughout the simulation for this base value. These can be observed in Fig. 6.

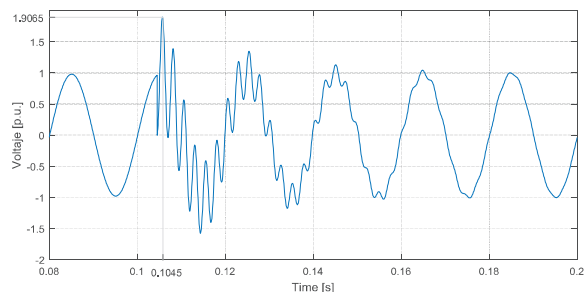


Fig. 5 Voltage response in p.u. for the worst case condition

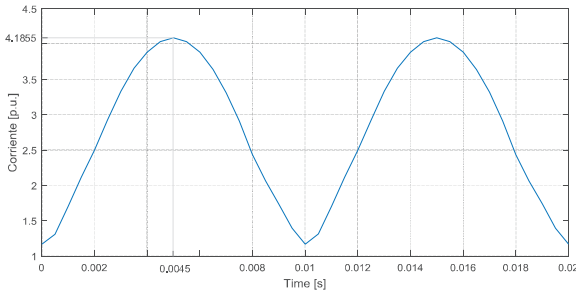


Fig. 6 Maximum p.u. currents obtained as a function of point-on-wave capacitor switching [7]

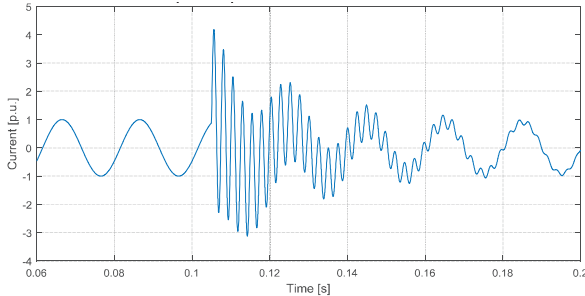


Fig. 7. Current response in p.u. for the worst case condition

According to Fig. 5 and Fig.7 values, the voltage and current transient responses can be really harmful for the system unless corrective actions are implemented.

C. Analytical calculation for the transient frequency response

Neglecting the reactance of the induction motors (with the aim of reducing the order system), the transient voltage frequency response at the 10 kV PCC is modelled into the frequency domain using the Laplace Transform. The equivalent circuit is presented in Fig. 8.

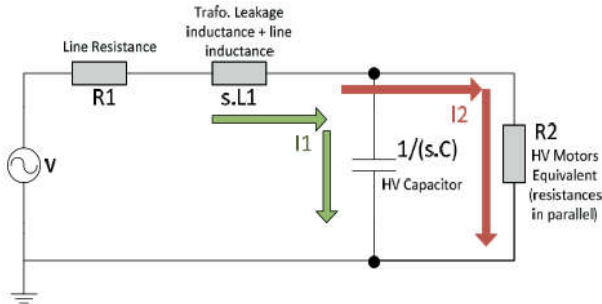


Fig. 8 Frequency domain equivalent circuit [8]

Using the mesh method, equation (11) – (13) is given by:

$$V = I_1 \left[R_2 + sL + \frac{1}{sC} \right] + I_2 [R_2 + sL] \quad (11)$$

$$V = I_1 [R_2 + sL] + I_2 [R_2 + R_1 + sL] \quad (12)$$

$$\begin{vmatrix} R_2 + sL + \frac{1}{sC} & R_2 + sL \\ R_2 + sL & R_2 + R_1 + sL \end{vmatrix} = 0 \quad (13)$$

Solving the determinant created, the system is given by a second order expression of equation (14):

$$s^2(R_1L) + s \left(R_1 + R_2 + \frac{L}{C} \right) + \frac{R_1 + R_2}{C} = 0 \quad (14)$$

Where, the roots of this equation are given by equation (15) and equation (16) presents the structure of the found roots.

$$s = -421.74 \pm j244.15 \quad (15)$$

$$s = \text{Real} \pm j(2\pi f) \quad (16)$$

Comparing terms, the resonant frequency is inferred, as can be observed in equation (17):

$$f = 388.57 \text{ Hz} \quad (17)$$

Hence, a detailed observation of the plot for the transient response of Fig. 9, the frequency is obtained as one over the observed period given a value of $1/0.0026 = 384 \text{ Hz}$, which is very close to the one obtained analytically (388.57 Hz); validating the mathematical approach performed previously.

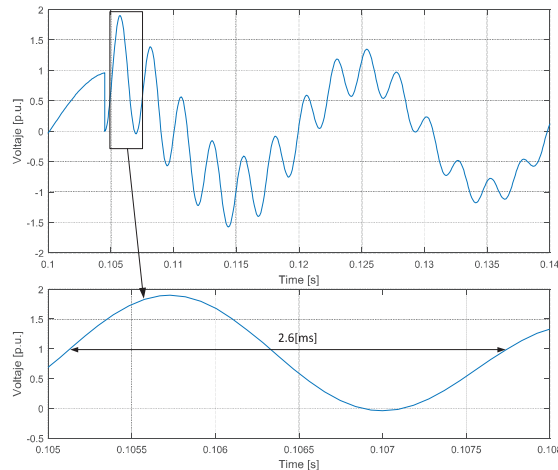


Fig. 9 Interface for the frequency on the transient voltage response

III. CASE ANALYSIS 2

The second case scenario considers the LV network in Operation (LV capacitor bank included), both of the HV induction motors are started. The HV capacitor bank is switched on in order to determine the maximum value for the transient overvoltage in conditions at the 400 V PCC [2],[9].

A. Electric System Model

The low voltage network side parameters will also be obtained to model the entire system. Notice that, using the transformation ratio ($R_t=25$), the parameters must be referred to the high voltage side to make an appropriate simulation into a total per-phase equivalent circuit basis.

Following similar criteria used in for the first motor analysed, the parameters of the high voltage are given by equation(18):

$$I_{\text{phase}} = \frac{P_{\text{phase}}}{V_{\text{phase}} \text{pf}} = 3849 \text{ A} \quad (18)$$

Thus, the phase load impedance (Zl) is expressed in equation (19):

$$Zl = \frac{V_{\text{phase}}}{I_{\text{phase}}} = 60 \text{ m}\Omega \quad (19)$$

As the power factor is 0.75 ($Zl=41.41^\circ$), the load resistance (R_1) and load reactance (X_1) are represented in equations (20) and (21):

$$R_1 = Z_1 * \cos(\varphi) = 45 \text{ m}\Omega \quad (20)$$

$$X_1 = Z_1 * \sin(\varphi) = 39.68 \text{ m}\Omega \quad (21)$$

The load inductance (L_1) is obtained by equation (22):

$$L1 = \frac{Xl}{2\pi f} = 126.325 \mu\text{H} \quad (22)$$

Transformer ratio relation is applied to refer the variables to the high voltage side, following equation (23) and (24):

$$Rl_{\text{HV}} = R_1 Rt^2 = 28.12 [\text{m}\Omega] \quad (23)$$

$$Ll_{\text{HV}} = L_1 Rt^2 = 78.95 [\text{mH}] \quad (24)$$

On the other side, the parameters of the low voltage capacitor are given following equations (25) – (27).

$$I_{\text{phase}_c} = \frac{Q_{\text{phase}_c}}{V_{\text{phase}} \sin(90^\circ)} = 2165.1 [\text{A}] \quad (25)$$

$$C_{\text{LV}} = \frac{I_{\text{phase}_c}}{2\pi f (V_{\text{phase}})} = 29.84 [\text{mF}] \quad (26)$$

$$C_{\text{LV}_{\text{HV}}} = C_{\text{LV}} \left(\frac{1}{Rt} \right)^2 = 47.74 [\mu\text{H}] \quad (27)$$

As the voltage reference used is 10 kV, no transformation ratio relation is needed for the leakage inductance of the transformer, this can be observed in equations (28) and (29).

$$X_{\text{TX}_8} = \frac{V_{\text{line}}^2}{S_{\text{SC}}} \epsilon_{\text{cc}} = 750 \text{ m}\Omega \quad (28)$$

$$L_{\text{TX}_8} = \frac{X_{\text{TX}_8}}{2\pi f} = 2.38 \text{ mH} \quad (29)$$

Considering Fig. 1, the low voltage line resistance and inductance will be $300 \mu\Omega$ and $0.9 \mu\text{H}$ respectively. These values must be referred to the high voltage side:

$$R_{\text{LV}_{\text{HV}}} = R_{\text{LV}} * Rt^2 = 187.5 \text{ m}\Omega \quad (30)$$

$$X_{\text{LV}_{\text{HV}}} = X_{\text{LV}} * Rt^2 = 562.5 \mu\text{H} \quad (31)$$

Figure 10 shows the complete per-phase equivalent circuit of the system using the calculated values.

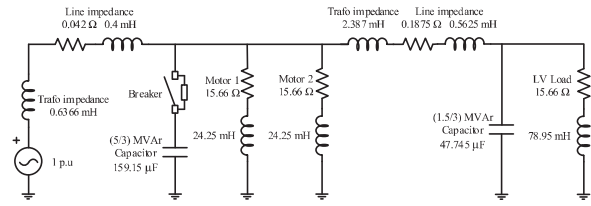


Fig. 10 Per-phase equivalent circuit of the complete system

B. Transient Voltage response

To obtain the highest transient overvoltage, same methodology that previous section is applied. This is performing 40 simulations representing the high voltage capacitor switching in steps of 0.5 ms from zero to 20 ms.

For this analysis, the end customer's voltage at the PCC for the low voltage side is the most important part, where the worst transient response found has a peak value of 2.4986 p.u. as is presented in Fig. 11.

The transient happens when the capacitor switching is done at a point on wave of 4.5 ms. Similarly, the highest possible current is shown in Fig. 12, which appears and it appears if the capacitor is connected at a point on wave of 5 ms and takes a value of 9.8261 p.u.

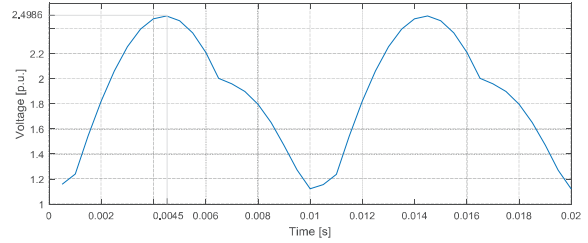


Fig. 11 Maximum p.u. voltages at the LV PCC as a function of point-on-wave capacitor switching

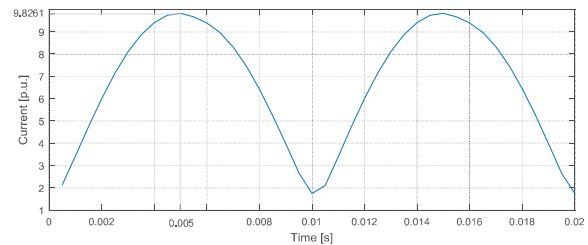


Fig. 12 Maximum p.u. currents at the LV PCC as a function of point-on-wave capacitor switching

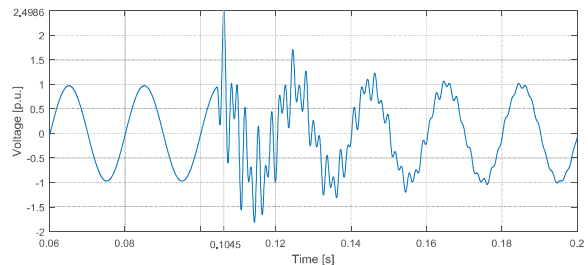


Fig. 13 Voltage response in p.u. at the LV PCC for the worst case condition

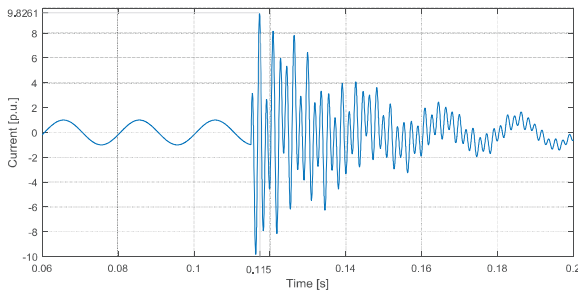


Fig. 14 Current response in p.u. at the LV PCC for the worst case condition

Furthermore, the particular responses for the worst-case condition for voltage and current are shown in Fig. 13 and Fig. 14.

IV. PROPOSED SOLUTIONS

Considering that the devices are connected as LV loads can withstand transient over voltages until 2 times the rated value. This work proposes two ways to solve the exposed problem.

As initially mentioned, there are two main ways to face this transient overvoltage phenomenon. These are the use of pre-insertion resistors and surge arresters.

The first option is to connect in parallel a breaker and a resistance with the capacitor switch. In this way, the chosen resistance is added during the start-up of the capacitor bank, which reduces the peak value of overvoltage and over current responses.

The scheme is shown in Fig. 15 which details the respective model implemented in Simulink-Matlab®. In first place, the HV capacitor is fed through the pre-insertion resistor using Breaker 2 (B2)[11]. After, an adequate amount of time (generally some milliseconds), Breaker 1 (B1) is switched on allowing a direct low-impedance connection for the capacitor bank.

Depending on the resistance value and the time in which Breaker 1 (B1) is turned on in simulation, there are different transient responses for the voltage and current at the LV PCC. Choosing a 15 Ω resistor and allowing current to go through it for 25 ms. until Breaker 1 is activated, a suitable voltage response at the LV PCC is reached. This response is far below the requested 2 p.u. limit. The performance of the proposed solution can be seen in Fig. 16 and Fig. 17 respectively.

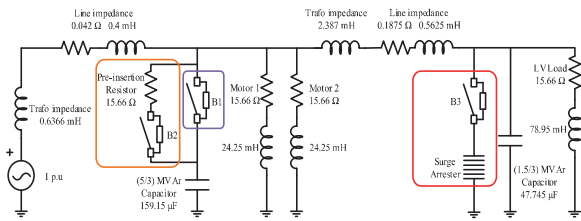


Fig. 75 Per-phase equivalent circuit in of the entire system including transient overvoltage solutions

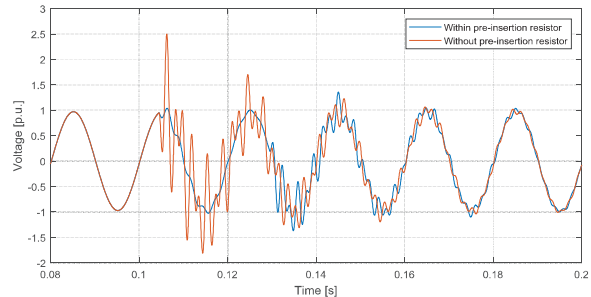


Fig. 16 Voltage response in p.u. for the worst case condition within and without a Pre-insertion resistor

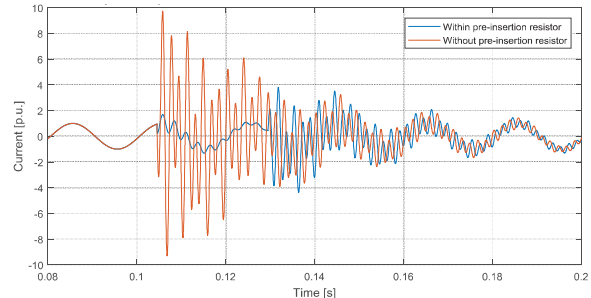


Fig. 17 Current response in p.u. for the worst case condition within and without a Pre-insertion resistor

On the other hand, the second solution consists on installing a surge arrester at the end-user PCC as in Fig. 15. The surge arrester is set up to limit the transient voltage below 2 p.u. Notice that Breaker 3 (B3) must always be connected because the surge arrester needs to be working all time. Keeping in mind that surge arresters have large MOV (Metal Oxide Varistor) blocks, which divert surge currents through varying its resistance when voltages above the rated value appear[12]. In Fig 18 and Fig. 19 is illustrated the performance of this device successfully in this case of analysis. As can be observed, the transient voltage and current responses are improved.

For the HV line, the frequency for the transient voltage response with no correction actions at the HV capacitor bank PCC is presented by equation (33):

$$f_2 = \frac{1}{2\pi\sqrt{L_2 C_2}} = 424.1 \text{ Hz} \quad (33)$$

In the same way, the natural frequency response for the voltage at the LV PCC is:

$$f_1 = \frac{1}{2\pi\sqrt{L_1 C_1}} = 391.82 \text{ Hz} \quad (33)$$

As the obtained frequency for the transient voltage at the HV capacitor is close to the frequency for the first LV, the transient in this last capacitor is amplified due to resonance[12]. This is the reason that bigger over voltages appears in the LV PCC, which was confirmed by the simulations carried out.

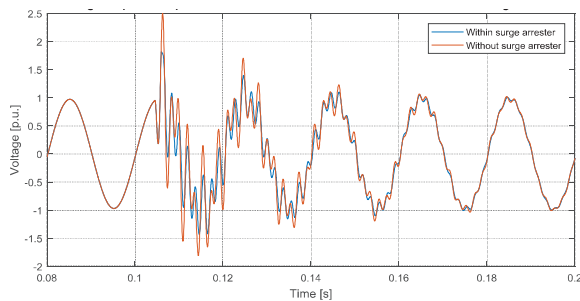


Fig. 18 Voltage response in p.u. for the worst case condition within and without a Surge Arrester

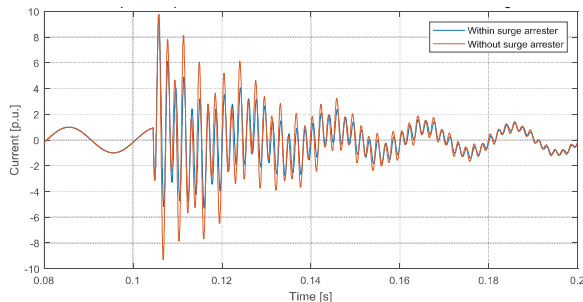


Fig. 19 Current response in p.u. for the worst case condition within and without a Surge Arrester

V. CONCLUSIONS

Transient overvoltages produced by the switching action of power-factor-correction capacitors have been studied in this report. This phenomenon can be harmful in electrical systems as it has been verified by simulation. For that reason, it is important to protect end user's loads against these threats by using solutions like pre-insertion resistors and surge arresters. If these devices are correctly calibrated, a normal operation in the load even when typical transient overvoltages take place is expected. Mitigate overvoltage phenomenon using capacitors gives more tools to affront the misoperation of a substantial part of the power system that involves important troubles.

VI. REFERENCES

- [1] Cano J, Unit 3- Transient Overvoltages Slides, EECPS Master, Gijón/Spain, Feb 2013
- [2] Domínguez X, Power Quality Practical Training: Transient Overvoltages
- [3] Martínez Juan, Transient Analysis of Power Systems: Solutions Techniques, Tools and Applications, First Edition, John Wiley and Sons, Ltd, 2015.
- [4] Expósito, A. G., Gomez-Exposito, A., Conejo, A. J., & Canizares, C. (Eds.). (2016). Electric energy systems: analysis and operation. CRC Press.
- [5] Huang, Z., Ni, Y., Shen, C. M., Wu, F. F., Chen, S., & Zhang, B. (2000). Application of unified power flow controller in interconnected power systems-modeling, interface, control strategy, and case study. *IEEE Transactions on Power Systems*, 15(2), 817-824.
- [6] Mendis, S. R., & Gonzalez, D. A. (1992). Harmonic and transient overvoltage analyses in arc furnace power systems. *IEEE transactions on industry applications*, 28(2), 336-342.
- [7] Mahseredjian, J., Dinavahi, V., & Martínez, J. A. (2009). Simulation tools for electromagnetic transients in power systems: Overview and challenges. *IEEE Transactions on Power Delivery*, 24(3), 1657-1669.
- [8] Belkhat, M., Edwards, J., Hoonchareon, N, Transients in Power Systems, School of Electrical and Computer Engineering Purdue University, TR-ECE 95-29, December 1995.
- [9] Kunder, Prabha, Power System Stability and Control, McGraw-Hill Inc., New York, 1994.
- [10] Pawar, V. S., & Shembekar, S. M. (2013). Transient Overvoltages in Power System. *International Journal of Science, Spirituality, Business and Technology (IJSSBT)*.
- [11] M. Beanland, T. Speas, J. Rostron, —Pre-insertion Resistors in High Voltage Capacitor Switching, — Western Protective Relay Conference, Oct. 19 – 21, 2004, Spokane, WA.
- [12] Crouse, Hinds, Lightning and surge protection – basic principles, Application note MTL surge protection, October 2016, EATON Powering Business Worldwide.
- [13] M. B. Marz, T. E. Royster, C. M. Wahlgren, —A Utility's Approach to the Application of Scout Arresters for Overvoltage Protection of Underground Distribution Circuits, —2994 IEEE Transmission and Distribution Conference Record, Chicago, April 1994

VII. BIOGRAPHY



X. Domínguez obtained his engineering degree in Electronics and Control at Escuela Politécnica Nacional (EPN) in Quito-Ecuador - 2010. The, he studied from 2012 to 2014 in Spain at Universidad de Oviedo, where he got his master's degree in Conversión de Energía Eléctrica y Sistemas de Potencia. Nowadays, he work as full time teacher at Universidad Técnica del Norte (Ibarra-Ecuador).

Areas of interest: Power electronics, Energy Quality and Industrial Control.



Israel Paredes, was born in Riobamba-Ecuador on June 24, 1988. He completed his high school studies at the Salesiano's High School "STAR". He graduated from the Escuela Politécnica Nacional in 2013 obtaining the degree of Electronics and Control Engineer. He is currently a teacher at the Escuela Politécnica Nacional and he is studying a master program in Automation and Industrial Electronic Control at the EPN.

Areas of interest: Industrial control, control systems and power electronics.



Nataly PozoViera was born in Pillaro-Ecuador on February 10, 1991. She studied at "Santo Domingo de Guzmán"-Ambato High School. In 2014 she obtained her degree as an Engineer in Electronics and Control at Escuela Politécnica Nacional. Next, she obtained her Master in Science's degree in Electrical Power in 2016, at Newcastle University - United Kingdom. Nowadays, Nataly works as Full Time Teacher in the Department of

Automation and Industrial Control - EPN. Areas of interest: Control drives, Power Electronics, Smart Grids, Power systems and Machine design,



María Trujillo was born in Riobamba-Ecuador on February 15, 1990. She completed his secondary studies at Santa Mariana de Jesús de Riobamba. She graduated from the Escuela Politécnica Nacional as an Engineer in Electronics and Control in 2014. She obtained her Master's degree in Biomedical Engineering in 2016 at Universidad Politécnica de Madrid in Spain. At the same time she works like an intern in the

Center for Biomedical Technology in the bio instrumentation area. Actually holds the position of Teacher in the Department of Automation and Industrial Control - EPN.

Areas of interest: computer vision, computer and networks, diagnostic assisted by computer, artificial intelligent, bio-instrumentation, bio-mechanic automation and industrial control.



Jorge Luis Medina Mora was born in Ambato-Ecuador on August 10, 1988. He completed his secondary studies at Instituto Tecnológico Superior Bolívar de Ambato. He graduated from the Escuela Politécnica Nacional as an Engineer in Electronics and Control in 2013. In 2015 he obtained a scholarship from the Ecuadorian Government to pursue his postgraduate studies and obtained his Master's degree in Electronic and Electrical Engineering in

2016 at The University of Sheffield in United Kingdom. Currently holds the position of Full Time Teacher in the Department of Automation and Industrial Control.

Areas of interest: control of electrical machines, power electronics, robotics, computer vision, computer and networks, embedded systems, automation and industrial control.



Andrés Cuaycal, was born in Quito-Ecuador on August 8, 1990. He completed his high school studies at Instituto Tecnológico Superior "Sucre". He graduated from the Escuela Politécnica Nacional in 2015 obtaining the degree of Electronics and Control Engineer. He worked as Laboratory Assistant for Embedded Systems and Electrical Circuits at Escuela Politécnica Nacional.

He has developed several applications in control systems emphasizing the three-phase motor scalar control, the control of a robotic arm with 6 degrees of freedom using inverse kinematics and the simulation and control of a hexacopter. He is currently a teacher at the Escuela Politécnica Nacional.

Areas of interest: Mobile robotics, embedded systems, control systems and power electronics.